

Facile solubilization of titanate nanobelts for nonlinear optical investigations

This content has been downloaded from IOPscience. Please scroll down to see the full text.

2010 Nanotechnology 21 185707

(<http://iopscience.iop.org/0957-4484/21/18/185707>)

View [the table of contents for this issue](#), or go to the [journal homepage](#) for more

Download details:

IP Address: 159.226.142.161

This content was downloaded on 22/10/2014 at 07:33

Please note that [terms and conditions apply](#).

Facile solubilization of titanate nanobelts for nonlinear optical investigations

Miao Feng¹, Hongbing Zhan^{1,3} and Lei Miao^{2,3}

¹ College of Materials Science and Engineering, Fuzhou University, 2 Xueyuan Road, Fuzhou 350108, People's Republic of China

² Key Laboratory of Renewable Energy and Gas Hydrate, Guangzhou Institute of Energy Conversion, Chinese Academy of Sciences, Nengyuan Road, Wushan, Tianhe District, Guangzhou 510640, People's Republic of China

E-mail: hbzhan@fzu.edu.cn and miaolei@ms.giec.ac.cn

Received 1 January 2010, in final form 25 February 2010

Published 14 April 2010

Online at stacks.iop.org/Nano/21/185707

Abstract

A homogeneously translucent titanate nanobelt (TNB) suspension was prepared through facile surface modification of pristine TNBs by polymer wrapping with poly(allylamine hydrochloride). The resultant TNB aqueous suspension was found to remain stable for months. The nonlinear optical (NLO) and optical limiting (OL) properties of the TNB suspension were then investigated. We found that the TNB suspension behaves totally differently at 532 and 1064 nm excitation in the nanosecond laser pulse regime. The sample displays remarkable NLO and OL effects at 532 nm, originating from nonlinear scattering. However, the NLO and OL effects are entirely diminished at 1064 nm due to the absence of near-resonant absorption and the subsequent thermal effect.

(Some figures in this article are in colour only in the electronic version)

1. Introduction

If lasers are to be widely used in daily life, the development of highly effective nonlinear optical (NLO) and optical limiting (OL) material systems for application in protection from strong laser radiation is very urgent [1]. Nanostructures, which are expected to show quantum size effects in at least one direction, are attracting increasing interest and are even being considered for potential applications as optical limiters. Up to now, a wide range of nanostructured materials including carbon black [2], carbon nanotubes (CNTs) [3, 4], metal nanostructures [5–7], semiconducting nanoparticles [8, 9] and most recently graphenes [10, 11], have been intensively studied to determine their NLO and OL performance. Several OL mechanisms, particularly nonlinear absorption (NLA), nonlinear scattering (NLS) and nonlinear refraction (NLR), have been found to dominate different kinds of OL materials [2–11].

Oxide semiconductors with high dielectric constants are good host candidates for NLO and OL applications [12, 13]. As typical wide band gap semiconductor materials with

high dielectric constants, protonated titanate and TiO₂ nanostructures constitute a promising new class of materials for optical applications. Due to their non-hollow anisotropic inorganic nanostructures, belt-shaped titanates need not be stabilized by any kind of incorporated templating material, and the synthetic requirements for their production are surprisingly flexible. On the other hand, the interesting physical and chemical properties of these strongly anisotropic materials quite often differ from those of the corresponding bulk material and those of isotropic nanoparticles. Therefore, these materials have become highly topical for chemists, physicists, and materials scientists.

Recently, titanate nanomaterials have been obtained by several methods (including a template method [14], an electrochemical anodic oxidation method [15], and a strongly alkaline hydrothermal treatment [16]), which pave the way for the wide use of titanate-based pigments, gas sensors, photocatalysts, and photoelectronic devices. Although the morphological forms of the titanate nanomaterials have not been carefully defined and used in the literature, four different morphologies of titanates were observed during synthesis of titanate nanomaterials by alkaline hydrothermal treatment. They are: nanotubes (I), nanosheets (II), nanorods

³ Authors to whom any correspondence should be addressed.

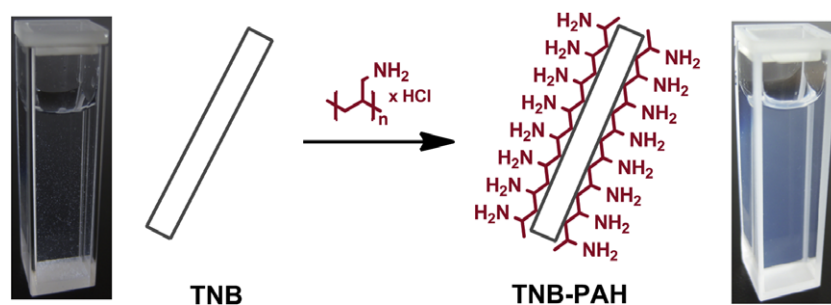


Figure 1. Schematic of functionalized TNBs with PAH in aqueous solution.

or nanowires (III), and nanofibers, nanoribbons, or nanobelts (IV) [17]. The specific morphologies of titanates can be adjusted by varying the condition of synthesis, for example temperature or the ratio of TiO_2 to NaOH [18–20]. The major advantages of alkaline hydrothermal TiO_2 for the fabrication of TiO_2 -based nanostructures [20, 21] are its simplicity, high transformation efficiency, and mass production. Most importantly, the nanobelts and nanotubes obtained by this method are single crystalline structures with good uniform diameter regardless of the various treatment conditions, which makes these materials more attractive for various applications (e.g. hydrogen storage [22], sensors [23, 24], batteries [25], electrochromism [26], photoluminescence [27], and dye-sensitized solar cells [28]).

It is well known that nano- TiO_x materials exhibit interesting optical properties and are also transparent over a large spectral range with a band gap around $E_g = 3.2$ eV. Thus several investigations have been carried out to study the NLO properties of these structures. In the past, the nonlinear refraction and absorption of TiO_2 thin film were analyzed using the Z-scan technique under 35 ps laser pulses at 532 nm [29] or the degenerate four-wave mixing technique under 70 ps pulse duration at 532 nm [30]. In particular, the effect of different phases of TiO_2 , rutile and anatase, on the NLO response were discussed [29]. Ganeev *et al* [31] studied the NLO properties of BaTiO_3 and SrTiO_3 nanoparticles using the 790 nm fs and ps pulses. However, the NLO effects and OL properties of titanate nanostructures have not been reported so far, probably due to severe aggregation caused by strong van der Waals interactions in a liquid environment. Therefore, the objectives of this study were to: (1) explore a facile route to the solubilization of titanate nanostructures, (2) investigate the NLO properties of titanate nanobelts (TNBs) using the Z-scan technique under 8 ns laser pulses at 532 nm, and (3) to explore their potential applications as optical limiters.

2. Experimental details

2.1. Sample preparation

TNB powders with a high aspect ratio were synthesized through hydrothermal reaction of TiO_2 powders with strong aqueous alkali (NaOH) solutions [32]. Typically, 1.8 g of commercial anatase TiO_2 powder of particle diameter 20 nm (Ishihara Sangyo, Kansai, ST-21) were dispersed in an aqueous

solution of NaOH (10 M, 100 ml) and charged into a Teflon-lined autoclave. The autoclave was oven-heated at 180 °C for 72 h. After having been washed thoroughly with distilled water and 0.1 M HCl aqueous solution, the obtained white cotton-batting-like solid was centrifugally separated and heat-treated at 400 °C in air for 5 h in order to get nanobelts with high crystal quality.

Poly(allylamine hydrochloride) (PAH) is a commercial cationic polyelectrolyte which has many applications, mostly related to modifying the flow and stability properties of aqueous solutions. For instance, they can be used to impart a surface charge to neutral nanoparticles, enabling them to be dispersed in aqueous solution [33, 34]. To obtain homogeneous and stable dispersions for NLO and OL measurements, we suspended the as-synthesized TNB powders (50 mg) in a NaCl aqueous solution (500 ml, 0.5 mol l^{-1}) containing PAH ($M_w \sim 56\,000$, 5 g l^{-1}), sonicated for 30 min in a high-power sonic bath, then stirred overnight at room temperature to ensure complete and uniform dispersal. The white precipitate collected by centrifugation of the suspension was washed several times with deionized water and ethanol. Then translucent TNB dispersions were obtained, which remained visually stable without precipitation for weeks. In contrast, the pristine TNBs entirely deposited at the bottom of the cell and therefore a totally transparent water solution was presented (figure 1).

2.2. Characterizations

The TNB materials were characterized through transmission electron microscopy (TEM; JEOL JEM-2010 microscope at an accelerating voltage of 200 kV), scanning electron microscopy (SEM; Philips Nova Nano SEM 230), x-ray diffraction (XRD; Philips XPert-MPD), UV-visible absorption spectroscopy (Shimadzu UV-2450 spectrometer), and photoluminescence (PL) spectrofluorophotometry (Deinburgh FL/FS TCSPC 920). Thermal properties were measured using a Q600 SDTTGA/DSC thermogravimetric analyzer under a N_2 flow rate of 100 ml min^{-1} at a heating rate of 10 °C min^{-1} .

2.3. NLO measurements

The NLO properties of the TNB suspensions were investigated by the open-aperture Z-scan technique using 8 ns pulses generated from a Q-switched Nd:YAG laser at wavelengths of

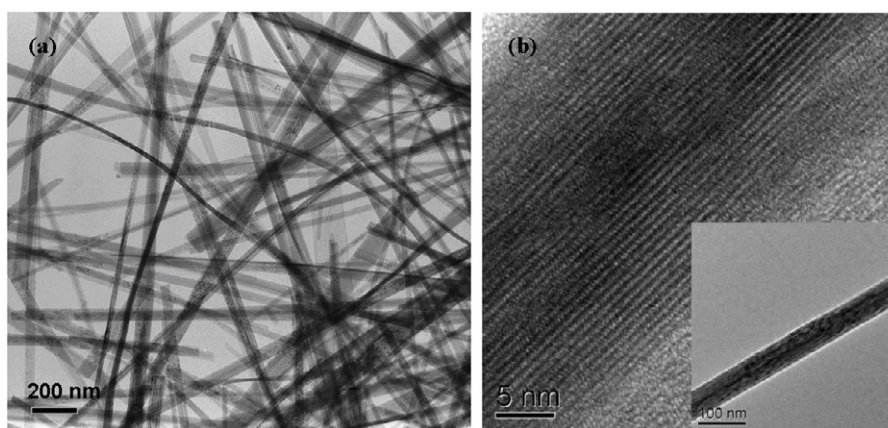


Figure 2. (a) Low-magnification TEM image of as-prepared TNBs. (b) HRTEM image of an individual TNB, exhibiting a well-resolved two-dimensional lattice. Inset: low-magnification of the TNB.

532 and 1064 nm. The laser pulses with 200, 500, and 1000 μJ energy for a single pulse were focused into a quartz cell of 5 mm path length with a spot size of $\sim 14.5 \mu\text{m}$ (532 nm) and $\sim 29.0 \mu\text{m}$ (1064 nm) at a 1 Hz repetition rate. During the experiments, the nanostructure suspensions were stirred regularly to refresh the samples at the laser illumination spot to avoid potential thermal or photoinduced shape transformation. We also checked the UV–visible absorption spectra of the samples before and after the experiments. No degradation of the UV–visible absorption spectra of the samples was observed, indicating there was no change in composition, shape, or size of the TNB nanostructures during the course of the experiments. The OL curves, which can be plotted as normalized transmission versus input fluence, were calculated from the open-aperture Z -scan data. In the nonlinear scattering (NLS) experiment, a fraction of scattered light was collected using a detector at $\sim 45^\circ$ horizontal to the direct incident beam. The linear transmittance of all tested samples was individually adjusted to $\sim 70\%$ at both the investigated wavelengths.

3. Results and discussion

Figure 2(a) shows the TNB sample consisting of a large quantity of nanobelts with lengths in the range of several hundred nanometers and widths of 40–80 nm. A typical high-resolution TEM image of the as-prepared TNBs is shown in figure 2(b), and the corresponding low-magnification bright field image is shown in the inset. The clearly resolved lattice image indicates that these TNBs are well crystallized. The low-magnification TEM image exhibits a belt-like structure exclusively. The titanate belt is long, smooth, and uniform with no sign of aggregation. The amine groups of PAH which have been functionalized on TNBs obviously ensure good separation and stability due to electrostatic interactions (repulsions) in aqueous solution. A SEM image of the TNB sample, as can be seen from figure 3, reveals that a network of nanobelt structures several micrometers long was formed after the hydrothermal process.

Figure 4 displays a typical XRD pattern and UV–visible absorption spectrum (inset) of the TNBs. The XRD pattern

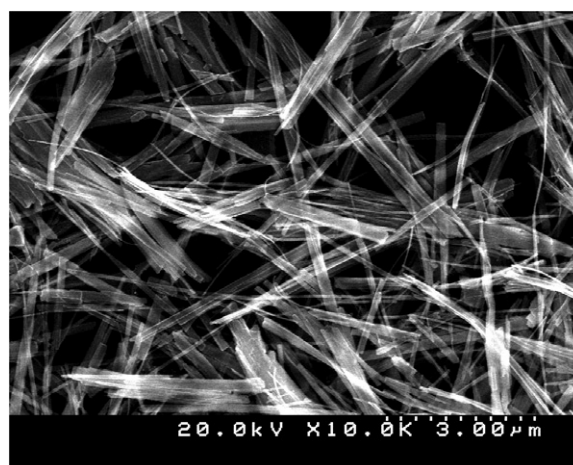


Figure 3. SEM image of the TNB sample.

features a prominent peak at $2\theta \sim 10^\circ$, reflecting a d spacing of 0.9 nm, which is a diagnostic gallery spacing for the layered protonic titanates. We denote here the apparent pattern of as-prepared nanobelts as the trititanate phase, having characteristic 2θ reflections of 10.2° , 25° , and 29.7° [35]. In combination with the x-ray emission spectroscopy (EDX) elemental analysis, TNBs can be identified as a layered titanate ($\text{Na}_x\text{H}_{2-x}\text{Ti}_3\text{O}_7$) structure. The UV–visible spectrum demonstrates absorption at around 300 nm that originated from the TNBs, which is characteristic of titanium oxide based materials [36].

Results of thermogravimetric analysis (TGA) further confirm the surface modification of TNBs by PAH. As shown in figure 5, both pristine TNB and modified TNB samples present a weight loss of 10% below 150°C , which is caused by the evaporation of physically adsorbed water. For modified TNBs, the subsequent additional loss of 5% ($400\text{--}450^\circ\text{C}$) is attributed to the decomposition of the PAH surfactant, and the residual weight of 85% is the weight of the bare TNBs. This indicates that the weight ratio of PAH to TNB is around 1:17. There is almost no weight loss after 450°C due to the excellent thermal stability of TNBs. Generally, titanate nanostructures

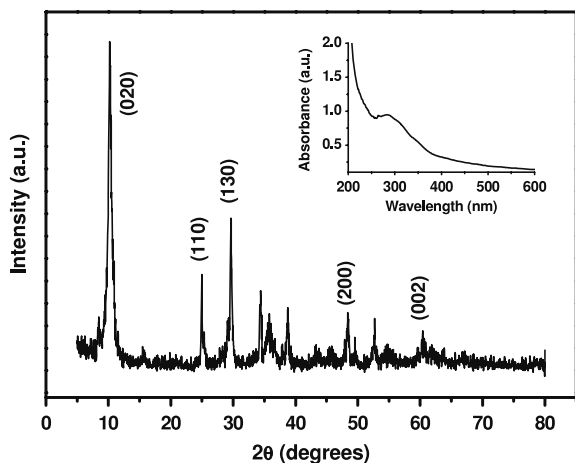


Figure 4. XRD pattern and UV-visible absorption spectrum (inset) of the TNBs.

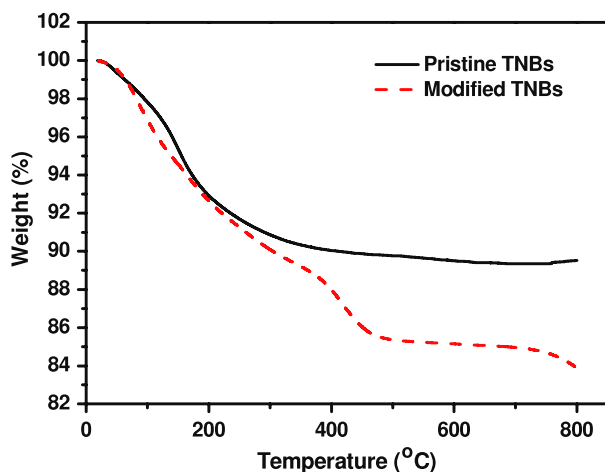


Figure 5. TGA thermograms of pristine and modified TNBs in flowing (100 ml min^{-1}) N_2 . The scan rate was $10^\circ\text{C min}^{-1}$.

are thermodynamically metastable phases, but nevertheless, the nanobelts have enhanced thermal stability compared with the ‘normal’ nanotubes because they lack an accessible inner volume [37]. However, the literature is not certain about the thermal stability of titanate nanostructures, due to various researchers analyzing titanate nanostructures having different aspect ratio, sodium content, history of preparation, and so forth. There is still a need for careful, systematic work in this area.

The Z-scan method, which measures the total transmittance through a sample as a function of incident laser fluence while the sample sequentially moves through the focus of a lens (along the z-axis), is a well-known technique to characterize the NLO properties of materials, including NLA, NLS, and NLR [38]. The Z-scan curves for the aqueous TNB suspension at 532 and 1064 nm excitation are shown in figures 6(a) and (b). At 532 nm, the sample exhibits a reduction in transmittance (valley) when it is near the laser beam focus, which is a typical feature of OL materials. The depth of the valley is a direct measure of the OL extent, and is different in the three

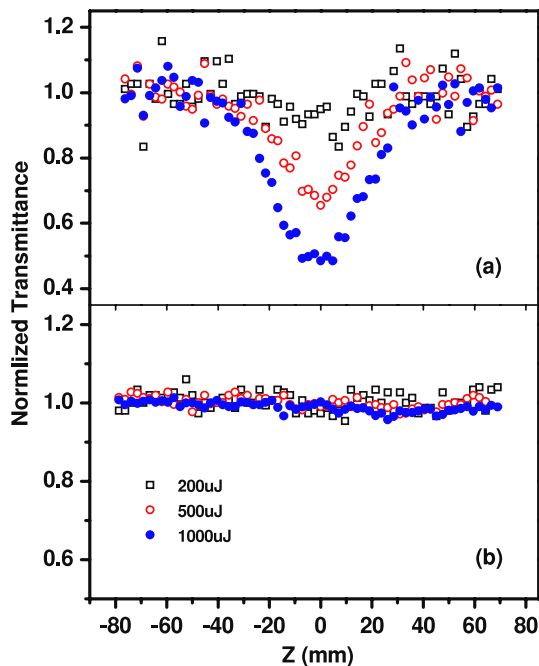


Figure 6. Z-scan curves for the aqueous TNB dispersion at 532 nm (a) and 1064 nm (b) excitation. Input energy for a single pulse: 200, 500, and 1000 μJ .

curves at different input energies of 200, 500, and 1000 μJ , with dips of ~ 0.8 , 0.6, and 0.45, respectively. It is interesting to note, however, that in the case of 1064 nm excitation, there are no signs of the reduction of transmittance, even at the highest input energy of 1000 μJ , indicating that there are no NLO effects at 1064 nm wavelength. This is very unlike the behaviors of CNTs and other nanostructured OL materials, where NLO and OL usually present at both 532 and 1064 nm excitations [2–11]. However, a similar phenomenon has been observed in bismuth nanorod suspensions [39].

Figure 7 black points show the variation of normalized transmittance versus input energy fluence for the TNB suspension at 532 nm. The transmittance is almost constant at low input fluence, and it starts to decrease as the irradiation exceeds 0.5 J cm^{-2} , displaying OL activity. To elucidate the possible NLO and OL mechanism for the TNB system, we carried out NLS measurements by collecting scattering signals at an angle of 45° to the propagation axis of the laser beam. The results are shown in the blue points of figure 7. The scattering signals are dominated by linear scatter at low input laser intensities, and they deviate from linear behavior as the input fluence exceeds a threshold value of $\sim 0.5 \text{ J cm}^{-2}$. Meanwhile, the contribution from NLS becomes larger with increasing laser fluence input, and it becomes the dominant contribution at high pump fluences. It should be noted that the onset of the decrease of transmittance is synchronous with the onset of the growth of scattering signals, implying that NLS is responsible for the NLO and OL behaviors. This is consistent with previous studies on CNTs and other nanostructured materials [2–11].

Two main mechanisms have been proposed to explain the NLO and OL behaviors of nanostructured materials:

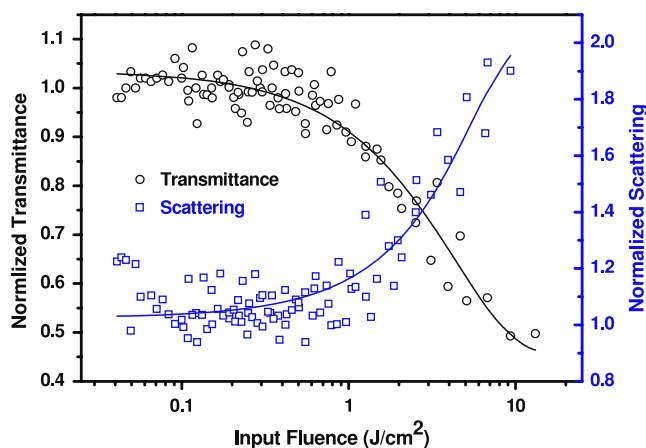


Figure 7. Nonlinear transmittance and scattering versus input fluence for the aqueous TNB dispersion at 532 nm excitation. The symbols denote the experimental data while the solid lines are guides to the eye.

NLA and NLS. Depending on the specific system, NLA may originate from two/multiphoton absorption, free carrier absorption, and reverse saturable absorption. NLS usually has two contributions. One is the photoinduced excitation, ionization, and expansion of the nanostructures, making them the scattering centers. The other contribution comes from solvent microbubble formation due to energy transfer, which acts as a second scattering center and leads to the further reduction in transmittance.

This NLS model can be further used to explain the presence of NLO and OL effects at 532 nm, and the absence at 1064 nm for the TNB system. As a semiconductor, the TNBs absorb energy via interband and intraband transitions. The presence of the absorption peak at around 300 nm (see the inset of figure 3) makes the absorption a ‘near-resonant’ process, resulting in localized heating and subsequent energy transfer to the surrounding medium through nonradiative de-excitation. At 1064 nm excitation, however, the absorption is too weak to create a strong-enough thermal effect, and therefore no scattering centers are formed. Furthermore, the propensity for scattering at 1064 nm is diminished by a factor of 16 when compared to 532 nm, considering the simple case of Rayleigh scattering where the scattering cross-section is proportional to λ^{-4} [38]. The disappearance of NLO and OL effects at 1064 nm for TNB applications implied that such single component TNBs cannot be used as a broadband optical limiters that would function in a multimechanistic fashion. Nevertheless, the NLO experimental data is still a good indication of the effectiveness of an optical limiting material for a nanosecond laser system at 532 nm.

Recently, the nonlinear refraction and absorption of BaTiO₃ and SrTiO₃ nanoparticles dissolved in ethylene glycol have been studied by using 790 nm fs and ps pulses [31]. The structural measurements have shown the sizes of the nanoparticles, which were greater than those at which one could expect the influence of quantum confinement processes. Since there are different varieties of metallic elements in titanate nanoparticles, and different experimental conditions

employed (i.e. experimental method, excitation wavelength and pulse duration), it is difficult to make any certain conclusions about the performance of titanate nanobelts and nanoparticles in the processes analyzed. Narrower nanostructure size distribution will benefit the conclusion of the role of the sizes on the nonlinear optical response of the material.

4. Conclusion

In summary, a stable TNB aqueous suspension was prepared through facile surface modification of pristine TNBs by polymer wrapping with PAH, and NLO and OL properties were investigated. We found that the TNB suspension behaves totally differently at 532 and 1064 nm excitations in the nanosecond laser pulse regime. The sample displays remarkable NLO and OL effects at 532 nm, which originated from the NLS; a very similar mechanism takes place in CNTs and other nanostructured materials. The NLO and OL effects are entirely diminished at 1064 nm due to the absence of near-resonant absorption and the subsequent thermal effect.

Acknowledgments

This work was supported by the Natural Science Foundation of Fujian Province (2009J01241) and the Fund of National Engineering Research Center for Optoelectronic Crystalline Materials (2005DC105003).

References

- [1] Crane R, Lewis K, Van Stryland E W and Khoshnevis M 1994 *Materials for Optical Limiting I, Proc. Material Research Society Symp.* vol 374 (Pittsburgh: Material Research Society)
- [2] Hood P, Pachter R, Lewis K, Perry J W, Hagan D and Sutherland R 1997 *Materials for Optical Limiting II, Proc. Material Research Society Symp.* vol 479 (Pittsburgh: Material Research Society)
- [3] Neto N M B, Mendonca C R, Misoguti L and Zilio S C 2004 *Appl. Phys. B* **78** 1
- [4] Chen Y et al 2007 *J. Nanosci. Nanotechnol.* **7** 1268
- [5] Chin K C et al 2006 *J. Mater. Res.* **21** 2758
- [6] Polavarapu L, Xu Q H, Dhoni M S and Ji W 2008 *Appl. Phys. Lett.* **92** 263110
- [7] Wang J and Blau W J 2009 *J. Opt. A: Pure Appl. Opt.* **11** 024001
- [8] Pan H et al 2006 *Appl. Phys. Lett.* **88** 223106
- [9] Jia W L, Douglas E P, Guo F G and Sun W F 2004 *Appl. Phys. Lett.* **85** 6326
- [10] Venkatram N, Rao D N and Akundi M A 2005 *Opt. Express* **13** 867
- [11] Xu Y F, Liu Z B, Zhang X L, Wang Y, Tian J G, Huang Y, Ma Y F, Zhang X Y and Chen Y S 2009 *Adv. Mater.* **21** 1275
- [12] Wang J, Hernandez Y, Lotya M, Coleman J N and Blau W J 2009 *Adv. Mater.* **21** 2430
- [13] Guan D Y, Chen Z H, Zhou Y L, Jin K J and Yang G Z 2006 *Appl. Phys. Lett.* **88** 111911
- [14] Iriraman L, Deepthy A, Krishnan B, Nampoore V P N and Radhakrishnan P 2008 *Appl. Phys. B* **90** 547
- [15] Liu S M, Gan L M, Liu L H, Zhang W D and Zeng H C 2002 *Chem. Mater.* **14** 1391
- [16] Gong D, Grimes C A, Varghese O K, Hu W, Singh R S, Chen Z and Dickey E C 2001 *J. Mater. Res.* **16** 3331

- [16] Kasuga T, Hiramatsu M, Hoson A, Sekino T and Niihara K 1998 *Langmuir* **14** 3160
- [17] Bavykin D V, Friedrich J M and Walsh F C 2006 *Adv. Mater.* **18** 2807
- [18] Bavykin D V, Parmon V N, Lapkin A A and Walsh F C 2004 *J. Mater. Chem.* **14** 3370
- [19] Tsai C C and Teng H 2004 *Chem. Mater.* **16** 4352
- [20] Ma R Z, Fukuda K, Sasaki T, Osada M and Bando Y 2005 *J. Phys. Chem. B* **109** 6210
- [21] Sun X M, Chen X and Li Y D 2002 *Inorg. Chem.* **41** 4996
- [22] Bavykin D V, Lapkin A A, Plucinski P K, Friedrich J M and Walsh F C 2005 *J. Phys. Chem. B* **109** 19422
- [23] Liu A, Wei M, Honma I and Zhou H 2005 *Anal. Chem.* **77** 8068
- [24] Liu A, Wei M, Honma I and Zhou H 2006 *Adv. Funct. Mater.* **16** 371
- [25] Gao X P, Lan Y, Zhu H Y, Liu J W, Ge Y P, Wu F and Song D Y 2005 *Electrochem. Solid-State Lett.* **8** A26
- [26] Tokudome H and Miyauchi M 2005 *Angew. Chem. Int. Edn* **44** 1974
- [27] Khan M A, Jung H T and Yang O B 2006 *J. Phys. Chem. B* **110** 6626
- [28] Varghese O K, Paulose M and Grimes C A 2009 *Nat. Nanotechnol.* **4** 592
- [29] Iliopoulos K, Kalogerakis G, Vernardou D, Katsarakis N, Koudoumas E and Couris S 2009 *Thin Solid Films* **518** 1174
- [30] Yu S W, Liao H B, Wen W J and Wong G K L 2005 *Opt. Mater.* **27** 1433
- [31] Ganeev R A, Suzuki M, Baba M and Kuroda H 2008 *J. Opt. Soc. Am. B* **25** 325
- [32] Miao L, Ina Y, Tanemura S, Jiang T, Tanemura M, Kaneko K, Toh S and Mori Y 2007 *Surf. Sci.* **601** 2792
- [33] Skirtach A G, Déjugnat C, Braun D, Susha A S, Rogach A L and Sukhorukov G B 2007 *J. Phys. Chem. C* **111** 555
- [34] Radziuk D, Shchukin D G, Skirtach A, Möhwald H and Sukhorukov G 2007 *Langmuir* **23** 4612
- [35] Horvath E, Kukovec A, Konya Z and Kiricsi I 2007 *Chem. Mater.* **19** 927
- [36] Ma R Z, Sasaki T and Bando Y 2004 *J. Am. Chem. Soc.* **126** 10382
- [37] Patzke G R, Krumeich F and Nesper R 2002 *Angew. Chem. Int. Edn* **41** 2446
- [38] Mansoor S B, Said A A, Wei T H, David J H and Stryland E W V 1990 *IEEE J. Quantum Electron.* **26** 760
- [39] Sivaramakrishnan S, Muthukumar V S, Sai S S, Venkataramaniam K, Reppert J, Rao A M, Anija M, Philip R and Kuthirummal N 2007 *Appl. Phys. Lett.* **91** 093104